Published for SISSA by Springer

Received: *July 22, 2014*
Revised: *September 28, 2014*
Accepted: *October 3, 2014*
Published: *October 20, 2014*

Statistical tests of sterile neutrinos using cosmology and short-baseline data

Johannes Bergström,[a] **M.C. Gonzalez-Garcia,**[b,c] **V. Niro**[a] **and J. Salvado**[d]

[a] *Departament d'Estructura i Constituents de la Matèria and Institut de Ciencies del Cosmos, Universitat de Barcelona, Diagonal 647, E-08028 Barcelona, Spain*

[b] *Institució Catalana de Recerca i Estudis Avançats (ICREA), Departament d'Estructura i Constituents de la Matèria and Institut de Ciencies del Cosmos, Universitat de Barcelona, Diagonal 647, E-08028 Barcelona, Spain*

[c] *C.N. Yang Institute for Theoretical Physics, State University of New York at Stony Brook, Stony Brook, NY 11794-3840, U.S.A.*

[d] *Wisconsin IceCube Particle Astrophysics Center (WIPAC) and Department of Physics, University of Wisconsin, Madison, WI 53706, U.S.A.*

E-mail: bergstrom@ecm.ub.edu, concha@insti.physics.sunysb.edu, niro@ecm.ub.edu, jordi.salvado@icecube.wisc.edu

Abstract: In this paper we revisit the question of the information which cosmology provides on the scenarios with sterile neutrinos invoked to describe the SBL anomalies using Bayesian statistical tests. We perform an analysis of the cosmological data in ΛCDM+r+ν_s cosmologies for different cosmological data combinations, and obtain the marginalized cosmological likelihood in terms of the two relevant parameters, the sterile neutrino mass m_s and its contribution to the energy density of the early Universe $\Delta N_{\rm eff}$. We then present an analysis to quantify at which level a model with one sterile neutrino is (dis)favoured with respect to a model with only three active neutrinos, using results from both short-baseline experiments and cosmology. We study the dependence of the results on the cosmological data considered, in particular on the inclusion of the recent BICEP2 results and the SZ cluster data from the Planck mission. We find that only when the cluster data is included the model with one extra sterile neutrino can become more favoured that the model with only the three active ones provided the sterile neutrino contribution to radiation density is suppressed with respect to the fully thermalized scenario. We have also quantified the level of (in)compatibility between the sterile neutrino masses implied by the cosmological and SBL results.

Keywords: Cosmology of Theories beyond the SM, Neutrino Physics

ArXiv ePrint: 1407.3806

doi:10.1007/JHEP10(2014)104

Contents

JHEP10(2014)104

1 Introduction

It is now an established fact that neutrinos are massive and leptonic flavors are not symmetries of Nature [1, 2]. In the last decade this picture has become fully established thanks to the upcoming of a set of precise experiments. In particular, the results obtained with solar and atmospheric neutrinos have been confirmed in experiments using terrestrial beams [3]. The minimum joint description of all these data requires mixing among all the three known neutrinos (ν_e, ν_μ, ν_τ), which can be expressed as quantum superposition of three massive states ν_i ($i = 1, 2, 3$) with masses m_i leading to the observed oscillation signals with $\Delta m^2_{21} = (7.5^{+0.19}_{-0.17}) \times 10^{-5}\,\mathrm{eV}^2$ and $|\Delta m^2_{31}| = (2.458 \pm 0.002) \times 10^{-3}\,\mathrm{eV}^2$ and non-zero values of the three mixing angles [4].

In addition to these well-established results, there remains a set of anomalies in neutrino data at relatively short-baselines (SBL) (see ref. [5] for a review) including the LSND [6] and MiniBooNE [7, 8] observed $\nu_\mu \to \nu_e$ transitions, and the $\bar{\nu}_e$ disappearance at reactor [9–11] and Gallium [12–14] experiments. If interpreted in terms of oscillations, each of these anomalies points out towards a $\Delta m^2 \sim \mathcal{O}(\mathrm{eV}^2)$ [15–23] and consequently cannot be explained within the context of the 3ν mixing described above. They require instead the addition of one or more neutrino states which must be *sterile*, i.e. elusive to Standard Model interactions, to account for the constraint of the invisible Z width which limits the number of light weak-interacting neutrinos to be 2.984 ± 0.008 [24].

Several combined analyses have been performed to globally account for these anomalies in addition to all other oscillation results in the context of models with one or two additional sterile neutrinos [20–23] with somehow different conclusions in what respects to the possibility of a successful joint description of all the data. Generically these global fits reveal a tension between disappearance and appearance results. But while refs. [21, 22] seem to find a possible compromise solution for 3+1 mass schemes, the analysis in ref. [23] concludes a significantly lower level of compatibility. In particular, ref. [21] concludes that a joint solution is found with

$$0.82 \leq \Delta m^2_{41} \leq 2.19 \text{ eV}^2 \text{ at } 3\sigma \tag{1.1}$$

$$|U_{e4}|^2 \sim 0.03\,, \qquad |U_{\mu 4}|^2 \sim 0.012\,.$$

Alternative information on the presence of light sterile neutrinos is provided by Cosmology as they contribute as extra radiation to the energy density of the early Universe which can be expressed as

$$\rho_R = \left[1 + \frac{7}{8}\left(\frac{4}{11}\right)^{4/3} N_{\text{eff}}\right] \rho_\gamma\,, \tag{1.2}$$

where ρ_γ is the photon energy density and the value of N_{eff} in the Standard Model (SM) is equal to $N^{\text{SM}}_{\text{eff}} = 3.046$ [25]. The presence of extra radiation is then usually quantified in terms of the parameter $\Delta N_{\text{eff}} \equiv N_{\text{eff}} - N^{\text{SM}}_{\text{eff}}$.

Sterile neutrinos contribute to ρ_R (i.e. to ΔN_{eff}) in a quantity which, in the absence of other forms of new physics, is a function of their mass and their mixing with the active neutrinos which determines to what degree they are in thermal equilibrium with those. In particular, in $3 + N_s$ scenarios with the values hinted by the SBL results (of the order of those in eq. (1)) the sterile neutrinos are fully thermalized (FT) and each one contributes to ρ_R as much as an active one (see for example [26, 27]), so

$$\Delta N^{3+N_s,FT}_{\text{eff}} = N_s\,. \tag{1.3}$$

Analyses of cosmological data have hinted for the presence of extra radiation, beyond the standard three active neutrinos since several years (see for example ref. [28] and references therein) and several authors have invoked the presence of eV-scale sterile neutrino as a plausible source of the extra radiation [29–33].[1] In the last four years the statistical significance of this extra radiation (or its upper bound) as well as the overall constraint on the neutrino mass scale has been changing as data from the Planck satellite [38], the Atacama Cosmology Telescope (ACT) [39], the South Pole Telescope (SPT) [40, 41], and most recently of the BICEP2 [42] experiment, has become available [43–50].

In particular, the recent measurement of B-mode signals from the BICEP2 [42] collaboration excludes a zero scalar-to-tensor ratio at 7σ and report a value of $r = 0.20^{+0.07}_{-0.05}$. This high value of r is compatible with previous results from the Planck data [38] if a running

[1] Alternative scenarios without sterile neutrinos have been proposed as well (see for example refs. [34–37] and references therein).

JHEP10(2014)104

of the scalar spectral index $dn_s/d\ln k$ is considered well beyond the characteristic value of 10^{-4} of slow-roll inflation models. Alternatively the tension might be eased by the presence of sterile neutrinos [44–48] without invoking such a large running of the scalar spectral index. It is important to remark that the BICEP2 analysis is based on dust polarization models that predicted subdominant contamination on their B-mode signal by dust polarization. Should the dust contamination be larger than assumed, the significance of their observation could be significantly reduced, see for example ref. [51]. Recently the Plank collaboration has released their results on the spectrum of polarized dust emission [52] which when extrapolated to the BICEP2 frequency seems to indicate that such higher contamination is possible. However, as stated in ref. [52], assessing the dust contribution to the B-model power spectrum measured by BICEP2 would require a joint analysis which is still lacking.

Since cosmological data have the potential to test regions of parameter space of the sterile neutrino scenarios invoked to account for the SBL anomalies, the question of to what degree they support them has received an increasing attention in the literature [33, 53–56]. The generic conclusion is that, in order to accommodate the cosmological observations within the $3+N_s$ scenarios motivated by SBL results, some new form of physics is required to suppress the contribution of the sterile neutrinos to the radiation component of the energy density at the CMB epoch with respect to the FT expectation, eq. (1.3). Among others, extended scenarios with a time varying dark energy component [31], entropy production after neutrino decoupling [57], very low reheating temperature [58], large lepton asymmetry [26, 59, 60], and non-standard neutrino interactions [61–63], have been considered. All these mechanisms have the effect of diluting the sterile neutrino abundance or suppressing the production in the early Universe.

In this paper we revisit the question of the information which cosmology provides on the sterile scenarios introduced to explain the SBL anomalies using precise Bayesian statistical tests which we briefly describe in section 2. Section 3 contains the results of our cosmological analysis in ΛCDM+$r+\nu_s$ cosmologies for three representative sets of cosmological data. With these results at hand we answer the question of *how much cosmological data favour or disfavour the scenario with sterile neutrino masses invoked by SBL anomalies, with respect to a model without sterile neutrinos?* in section 4, and we do so in terms of the departure from the fully thermalized expectation, eq. (1.3). We also discuss the consistency of sterile parameter constrains implied by cosmology and SBL. In section 5 we summarize our conclusions.

2 The statistical framework

2.1 Model comparison

Bayesian inference is a rigorous framework for inferring which set of models or hypotheses H_i, are favoured by a data set $\mathbf{D}$. Bayes' theorem is used to calculate the probabilities of each of the hypotheses after considering the data, the *posterior probabilities*,

$$\Pr(H_i|\mathbf{D}) = \frac{\Pr(\mathbf{D}|H_i)\Pr(H_i)}{\Pr(\mathbf{D})}. \tag{2.1}$$

JHEP10(2014)104

Here $\Pr(\mathbf{D}|H_i)$ is the probability of the data, assuming the model H_i to be true, while $\Pr(H_i)$ is the *prior probability* of H_i, which is how plausible H_i is before considering the data. Considering especially the case of a discrete set of models, one can compare two of them by calculating the ratio of posterior probabilities, the *posterior odds*, as

$$\mathcal{O}_{ij} = \frac{\Pr(H_i|\mathbf{D})}{\Pr(H_j|\mathbf{D})} = \frac{\Pr(\mathbf{D}|H_i)}{\Pr(\mathbf{D}|H_j)} \frac{\Pr(H_i)}{\Pr(H_j)} = B_{ij} \frac{\Pr(H_i)}{\Pr(H_j)}. \tag{2.2}$$

In words, the posterior odds is given by the *prior odds* $\Pr(H_i)/\Pr(H_j)$ multiplied by the *Bayes factor* $B_{ij} = \Pr(\mathbf{D}|H_i)/\Pr(\mathbf{D}|H_j)$, which quantifies how much better H_i describes that data than H_j. The prior odds quantifies how much more plausible one model is than the other a priory, i.e., without considering the data. If there is no reason to favour one of the models over the other, the prior odds equals unity, in which case the posterior odds equals the Bayes factor.

For a model H, containing the continuous free parameters $\mathbf{\Theta}$, $\Pr(\mathbf{D}|H)$ also called *evidence* of the model is given by

$$\begin{aligned} \Pr(\mathbf{D}|H) = \\ \int \Pr(\mathbf{D}, \mathbf{\Theta}|H) \mathrm{d}^N\mathbf{\Theta} &= \int \Pr(\mathbf{D}|\mathbf{\Theta}, H) \Pr(\mathbf{\Theta}|H) \mathrm{d}^N\mathbf{\Theta} \\ &= \int \mathcal{L}(\mathbf{\Theta}) \pi(\mathbf{\Theta}) \mathrm{d}^N\mathbf{\Theta}. \end{aligned} \tag{2.3}$$

Here, the *likelihood function* $\Pr(\mathbf{D}|\mathbf{\Theta}, H)$ is the probability (density) of the data as a function of the assumed free parameters, which we often denote by $\mathcal{L}(\mathbf{\Theta})$ for simplicity. The quantity $\Pr(\mathbf{\Theta}|H)$ is the correctly normalized prior probability (density) of the parameters and is often denoted by $\pi(\mathbf{\Theta})$. The assignment of priors is often far from trivial, but an important part of a Bayesian analysis.

From eq. (2.3), we note that the evidence is the average of the likelihood over the prior, and hence this method automatically implements a form of *Occam's razor*, since usually a theory with a smaller parameter space will have a larger evidence than a more complicated one, unless the latter can fit the data substantially better.

Bayes factors, or rather posterior odds, are usually interpreted or "translated" into ordinary language using the so-called *Jeffreys scale*, given in table 1, where "log" is the natural logarithm. This has been used in applications such as refs. [64–66] (and refs. [67, 68] in neutrino physics), although slightly more aggressive scales have been used previously [69, 70].

2.2 Parameters of interest and the marginal likelihood

In Bayesian statistics if one assumes a particular parametrized model to be correct, the complete inference of the parameters of that model is given by the posterior distribution through Bayes' theorem

$$\Pr(\mathbf{\Theta}|\mathbf{D}, H) = \frac{\Pr(\mathbf{D}|\mathbf{\Theta}, H) \Pr(\mathbf{\Theta}|H)}{\Pr(\mathbf{D}|H)} = \frac{\mathcal{L}(\mathbf{\Theta}) \pi(\mathbf{\Theta})}{\Pr(\mathbf{D}|H)}. \tag{2.4}$$

JHEP10(2014)104

$\lvert\log(\text{odds})\rvert$	odds	$\Pr(H\lvert\mathbf{D})$	Interpretation
< 1.0	$\lesssim 3:1$	$\lesssim 0.75$	Inconclusive
1.0	$\simeq 3:1$	$\simeq 0.75$	Weak evidence
2.5	$\simeq 12:1$	$\simeq 0.92$	Moderate evidence
5.0	$\simeq 150:1$	$\simeq 0.993$	Strong evidence

Table 1. Jeffrey's scale often used for the interpretation of model odds. The posterior model probabilities for the preferred model H are calculated by assuming only two competing hypotheses.

We see that the evidence here appears as a normalization constant in the denominator. Since the evidence does not depend on the values of the parameters $\mathbf{\Theta}$, it is usually ignored in parameter estimation problems and the parameter inference is obtained using the unnormalized posterior.

For the case in which we have only a subset of parameters of interest, λ, so $\mathbf{\Theta} = (\lambda, \eta)$, where η denotes the *nuisance parameters*,

$$P(\lambda, \eta) = \Pr(\lambda, \eta|\mathbf{D}, H) \propto \mathcal{L}(\lambda, \eta)\pi(\lambda, \eta)\,, \tag{2.5}$$

and the inference on λ is obtained by marginalizing over the nuisance parameters in the usual way

$$P(\lambda) = \int P(\lambda, \eta)\mathrm{d}\eta\,, \tag{2.6}$$

with no need to ever consider a likelihood $\mathcal{L}(\lambda)$ depending only on the parameter of interest. This is typically unproblematic in the case where the data is sufficiently informative to eliminate all practical prior dependence. Often, however, this is not the case, and there can be large dependence on the prior chosen. In this case one can consider as a partial step the marginal likelihood function

$$\mathcal{L}(\lambda) = \int \mathcal{L}(\lambda, \eta)\pi(\eta)\mathrm{d}\eta\,, \tag{2.7}$$

such that $P(\lambda) \propto \mathcal{L}(\lambda)\pi(\lambda)$.

This likelihood function then encodes the information on λ contained in the data (under H and after taking into account the uncertainty on the nuisance parameters), without needing to specify a prior $\pi(\lambda)$. Note that, since the marginal likelihood is not a probability density, it is not normalized to unity, and is not sufficient to perform the full inference. Also, it is generally different from the profile likelihood, i.e., the likelihood maximized (rather than integrated) over the nuisance parameters. Hence, regions defined by $-2\log(\mathcal{L}(\lambda)/\mathcal{L}^{\max}) < C$ will not, in general, be the same as those using the profile likelihood, although arguments justifying defining regions in this way for profile likelihoods typically also apply to marginal likelihoods. As shown in ref. [71], the profile and marginal likelihoods are indeed similar for the cosmological data and models considered there. In any case, the marginal likelihood can still be useful in scientific reporting as a rough guide to what information the data contains, for example, by considering regions defined by $-2\log(\mathcal{L}(\lambda)/\mathcal{L}^{\max}) < C$ [72].

JHEP10(2014)104

Furthermore, if two data sets do not share any common nuisance parameters, the two marginal likelihoods can simply be multiplied to obtain the total marginal likelihood. Notice, however, that the marginal likelihood still depends on the priors on the nuisance parameters. If the nuisance parameters are well-constrained this dependence will be small, but in cosmology this is necessarily not always the case.

3 Cosmological analysis

3.1 Data sets

In our cosmological analysis, we use data on Cosmic Microwave Background, large scale structure (LSS) baryon acoustic oscillations (BAO) measurements, Hubble constant H_0, and galaxy cluster counts. In particular, we define the following data combinations:

- CMB: it includes the current Planck data [38] of the temperature anisotropy up to $l = 2479$, the high multipole values (highL), coming from ACT [39] and SPT data [40, 41], that covers respectively the $500 < l < 3500$ and $600 < l < 3000$ range, and the EE and TE polarization data from WMPA9 [73] (WP). It also includes the CMB lensing potential (lensing) reconstructed by the Planck collaboration [38] through the measurement of the four-point function.

- BAO: it includes the Data Release 11 (DR11) sample of the recent measurements by the BOSS collaboration [74]. The DR11 sample is the largest region of the Universe ever surveyed, covering roughly 8500 square degrees, with a redshift range $0.2 < z < 0.7$. The measure of the sound horizon at the drag epoch has been evaluated at redshift z=0.32 and at z=0.57, finding values in agreement with previous BAO measurements.[2]

- BICEP2: the 9 channels of the CMB BB polarization spectrum recently released by the BICEP2 experiment [42].

- HST: the data from the Hubble Space Telescope [79] on H_0, obtained through the distance measurements of the Cepheids:

$$H_0 = (73.8 \pm 2.4) \text{ km s}^{-1}\text{Mpc}^{-1} . \tag{3.1}$$

- PlaSZ: the counts of rich cluster of galaxies from the sample of Planck thermal Sunyaev-Zel'Dovich catalogue [80]. It constrains the combination $\sigma_8(\Omega_m/0.27)^{0.3} = 0.782 \pm 0.010$,[3]

[2]We have verified that the inclusion of the previous determinations of the BAO from the Sloan Digital Sky Survey (SDSS) Data Release 7 (DR7) [75, 76], the 6dF Galaxy Survey (6dFGS) [77], and WiggleZ measurements ref. [78] does not affect our results and therefore for the sake of simplicity we have not included them in the analysis. Indeed, for either of the analysis of the three data sets to be presented below, the main effect of the inclusion of the BAO data is to somewhat reduce the ranges of all fitted parameters but it does not substantially *shift* them, and hence it does not play any major role on our final conclusions.

[3]For simplicity we do not include the cosmic shear data of weak lensing from the Canada-French-Hawaii Telescope Lensing Survey (CFHTLenS) which constraints $\sigma_8(\Omega_m/0.27)^{0.46} = 0.774 \pm 0.040$, [81–83]. Although the combinations constrained by PlaSZ and CFHTLenS are not the same, given the much better precision of the PlaSZ data, the impact of including CFHTLenS in our analysis is very small.

JHEP10(2014)104

In order to test the dependence of our results on the inclusion of the recent BICEP2 data and on the tension with local HST and cluster PlaSZ results we perform the analysis with three different combinations of the data sets above that we label:

- *DATA SET 1:* CMB+BAO, where, as described above, CMB = Planck + WP + highL + lensing data, and BAO=DR11.
- *DATA SET 2:* CMB + BAO + BICEP2. We add to the previous data set, the results from BICEP2.
- *DATA SET 3:* CMB + BAO + BICEP2 + HST + PlaSZ. We add to the previous data set the results from HST and Planck SZ counts of galaxy clusters.

3.2 Cosmological model

We consider in our analysis a ΛCDM cosmology extended with a free scalar-to-tensor ratio, and three active plus one sterile neutrino species with a hierarchical neutrino spectra of the 3+1 type which we denote as ΛCDM+$r+\nu_s$. In this case the three active neutrinos have masses $m_{i=1,3} \lesssim \sqrt{|\Delta m^2_{31}|}$ while the forth sterile neutrino has a mass $m_4 \equiv m_s$.

As mentioned in the introduction, in the absence of other form of new physics the contribution of the sterile neutrino to the energy density is completely determined by its mass and its mixing with the active neutrinos. However in extended scenarios this may not be the case. So generically we will consider that in the 3+1 scenario, irrespective of m_s and mixings, the sterile neutrino contributes to ρ_R as

$$\Delta N_{\rm eff} \equiv F_{\rm NT}\, \Delta N_{\rm eff}^{3+1,FT} = F_{\rm NT} \tag{3.2}$$

where $F_{\rm NT}$ is an arbitrary quantity which quantifies the departure from the fully-thermalized active-sterile neutrino scenario and which we will consider to be independent of T in the relevant range of T in the analysis. So in what follows we will label as $\Delta N_{\rm eff} \equiv F_{\rm NT}$ this parameter.

The effect of m_s is included in the analysis via the effective parameter

$$m_{\rm eff} = (94.1\ {\rm eV})\ \Omega_s h^2\,, \tag{3.3}$$

with being h the reduced Hubble constant and $\Omega_s \equiv \rho_s/\rho_c$, with ρ_s the sterile neutrino energy density and ρ_c the current critical density. This effective mass is not equal to the physical mass m_s in general, and their relation depends on the assumed phase-space distribution of the sterile neutrinos. For thermally distributed sterile neutrinos characterized by a temperature T_s (in general different from the temperature of the active neutrinos T_ν)

$$m_{\rm eff} = (\Delta N_{\rm eff})^{3/4} m_s\,, \tag{3.4}$$

while if they are produced by non-resonant oscillations (the so-called Dodelson-Widrow scenario) (DW) [84] the resulting phase-space distribution of the sterile neutrinos is equal to that of the active neutrinos up a constant factor. In this case

$$m_{\rm eff} = \Delta N_{\rm eff} m_s\,. \tag{3.5}$$

JHEP10(2014)104

Parameter	Prior
$\Omega_b h^2$	$0.005 \to 0.1$
$\Omega_c h^2$	$0.001 \to 0.99$
Θ_s	$0.5 \to 10$
τ	$0.01 \to 0.8$
$\ln[10^{10} A_s]$	$2.7 \to 4$
n_s	$0.9 \to 1.1$
r	$0 \to 1$
$m_{\rm eff}$	$0 \to 3$
$N_{\rm eff}$	$3.046 \to 6$

Table 2. Uniform priors for the cosmological parameters considered in the analysis. The active neutrinos have been fixed to one massive with a mass of 0.06 and two massless. In addition, following ref. [38], an upper constraint on m_s, defined in eq. (3.4), of 10 eV is imposed, which roughly defines the region where the sterile neutrinos are distinct from cold or warm dark matter.

Altogether our analysis contain nine free parameters

$$\{\omega_b, \omega_c, \Theta_s, \tau, \log[10^{10} A_s], n_s, r, m_{\rm eff}, N_{\rm eff}\}\,, \tag{3.6}$$

where $\omega_{\rm b} \equiv \Omega_{\rm b} h^2$, $\omega_{\rm c} \equiv \Omega_{\rm c} h^2$ being the physical baryon and cold dark matter energy densities, $\Theta_{\rm s}$ the ratio between the sound horizon and the angular diameter distance at decoupling, τ is the reionization optical depth, $A_{\rm s}$ the amplitude of primordial spectrum, $n_{\rm s}$ the scalar spectral index, and r the scalar-to-tensor ratio. To generate the marginalized likelihoods we use the CosmoMC package [85], implemented with the Boltzmann CAMB code [86].

The parameters in (3.6) are assigned uniform priors with limits as given in table 2. Since we are interested in the constraints on sterile neutrino parameters, we follow section 2.2, and aim to evaluate the marginal likelihoods of $(m_{\rm eff}, N_{\rm eff})$, which will then be used for the tests presented in section 4. Thus in this analysis we consider $\{\omega_{\rm b}, \omega_{\rm c}, \Theta_{\rm s}, \tau, \log[10^{10} A_{\rm s}], n_{\rm s}, r\}$ as the *cosmological nuisance parameters*.[4] Note that we have employed uniform priors on $m_{\rm eff}$ and $N_{\rm eff}$ in the numerical analysis but that the marginal likelihoods to be presented below do not depend on the priors, since these are "factorized out". Furthermore, since the nuisance parameters are rather well-constrained the precise vales of the limits in table 2 do not not affect any results, and also employing different shapes on these parameters would have a small impact. The exception is r which is not so well-constrained (especially for certain data sets) and for which the physical lower limit is important.

[4] We do not include the lensing amplitude $A_{\rm L}$ as a free nuisance parameter, even when adding the local measurements on σ_8 and Ω_m, for which a significant deviation from the standard value of unity is preferred. We have checked that adding $A_{\rm L}$ only slightly shifts the preferred region for $m_{\rm eff}$ to higher values.

JHEP10(2014)104

3.3 Marginal cosmological likelihoods

The results of our analysis for the three data set combinations described in section 3.1 are shown in figures 1 and 2.

In the upper left panel of figure 1 and in the left panels of figure 2 we plot the contours of the marginal likelihood $\mathcal{L}(N_{\rm eff}, m_{\rm eff})$ normalized to the value of $\mathcal{L}(\Delta N_{\rm eff} = 0)$ (which does not depend on $m_{\rm eff}$).[5] The red contour delimits the regions for which m_s in eq. (3.4) exceeds 10 eV for which the sterile states becomes indistinguishable from cold or warm dark matter [38] and hence, for values of the parameters below the curve, the marginal likelihood is not evaluated. Black dashed contours are those of $-2\log(\mathcal{L}/\mathcal{L}^{\rm max}) < 2.30, 6.18, 11.83$, nominally corresponding to the 1σ, 2σ, and 3σ levels in two dimensions.

In the upper right panel of figure 1 and the right panels of figure 2 we show the contours of the marginal likelihood of $(N_{\rm eff}, m_s)$ for thermally distributed sterile neutrinos, while in the lower left panel of figure 1 we show the corresponding marginal likelihood in the DW scenario. We see that for both DW and thermal ν_s scenarios, m_s becomes increasingly large for decreasing $\Delta N_{\rm eff}$, hence the distinctive appearance of large "flat" regions and weak constraints on $m_{\rm s}$ for small $\Delta N_{\rm eff}$. Also as seen in figure 1 the results for the DW and the thermal ν_s scenarios are qualitatively very similar. Only, since for fixed $m_{\rm eff}$ and $\Delta N_{\rm eff}$, $m_s^{\rm DW} = m_s^{\rm TH}\Delta N_{\rm eff}^{-1/4}$, for $\Delta N_{\rm eff} \leq 1$ the likelihood contours in the DW scenario are shifted to slightly larger masses in an amount which decreases as $\Delta N_{\rm eff}$ increases.

The impact of BICEP2 data can be seen by comparing the upper panels in figure 1 and figure 2. The addition of BICEP2 data gives a preference for large values of the tensor-to-scalar ratio r and, due to its correlation with $\Delta N_{\rm eff}$, therefore leads to the shift to slightly larger values of $\Delta N_{\rm eff}$ observed in upper panels in figure 2. Since r is now better constrained, also the preferred region becomes slightly smaller.

The effects of adding HST+PlaSZ in the analysis are displayed in the lower panels in figure 2 where we see a shift to larger values of both $\Delta N_{\rm eff}$ and $m_{\rm eff}$. This is so because the constraints on σ_8 of the PlaSZ measurement, which are in tension with the other experiments within this model, can be somewhat alleviated by an increase in $m_{\rm eff}$, while the inclusion of HST yields an increase in $\Delta N_{\rm eff}$.

All these results are in qualitative agreement with those in the analyses in refs. [44–50]. However we notice that by showing the marginal likelihood we are explicitly not assigning any priors to the sterile parameters. This is an advantage in the absence of a physical motivation for them, especially $m_{\rm s}$, since the data at hand is expected to leave a large prior dependence. For example, if one used a prior on $m_{\rm s}$ which is uniform in $\log m_{\rm s}$ instead of in $m_{\rm s}$, as in general the likelihood is non-negligible for a vanishing sterile mass, the derived Bayesian constraints on $m_{\rm eff}$ and $\Delta N_{\rm eff}$ would be very different. In principle one could embark on an extensive prior sensitivity analysis, but in this work we will instead focus on analyses for which the results have little or no prior dependence. Notice also that the present analysis are done in the context of a cosmological constant parametrization of the dark energy contents of the Universe. However, we have verified that a general equation

[5] For likelihoods more than eight log-units away from the maximum value, we extrapolate using a constant value. It could be made more accurate by using non-constant functions such as polynomials but no qualitative change is expected.

JHEP10(2014)104

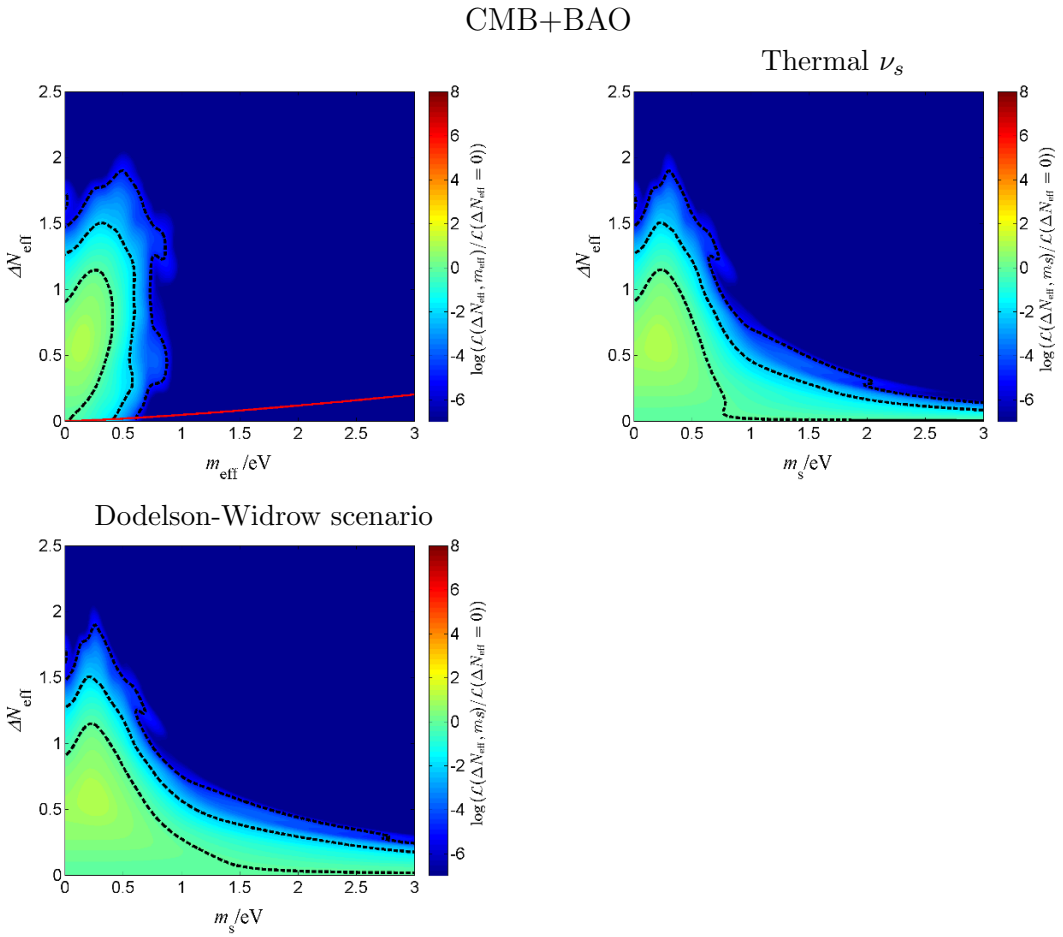

Figure 1. Marginal likelihood of $(m_{\rm eff}, \Delta N_{\rm eff})$ (upper right panel) and of $(m_s, \Delta N_{\rm eff})$ for thermally distributed ν_s (upper left panel) and for the for DW scenario (lower panel) for the CMB+BAO cosmological data set (*SET 1*). Black dashed contours are those of $-2\log(\mathcal{L}/\mathcal{L}^{\rm max}) < C$, which would correspond to nominal 1,2,3 sigma levels. The red line denotes the region for which $m_s = 10\,{\rm eV}$ for thermal ν_s.

of state of dark energy, $\omega \neq -1$, results only in a slight relaxation of the upper bound on the sterile mass, while it has a rather marginal impact on the determination of $\Delta N_{\rm eff}$, see also ref. [87]. Hence, the main conclusions of the compatibility between the cosmological and SBL results, which we discuss in the following, would remain valid even in that case.

Finally, in order to better illustrate how the constraints depend on the sterile mass we plot in figure 3, the slices of the marginal likelihood as a function of m_s for fixed $\Delta N_{\rm eff}$. Also shown in the figure is the marginal likelihood for the SBL analysis in the 3+1 scenario (marginalized with respect to the lighter neutrino masses and all mixings) as given in figure 1 in ref. [54].

4 Test on sterile neutrinos models

In this section we perform the statistical tests on the 3+1 scenarios invoked to explain the SBL anomalies using the results of the cosmological analysis presented in the previous

JHEP10(2014)104

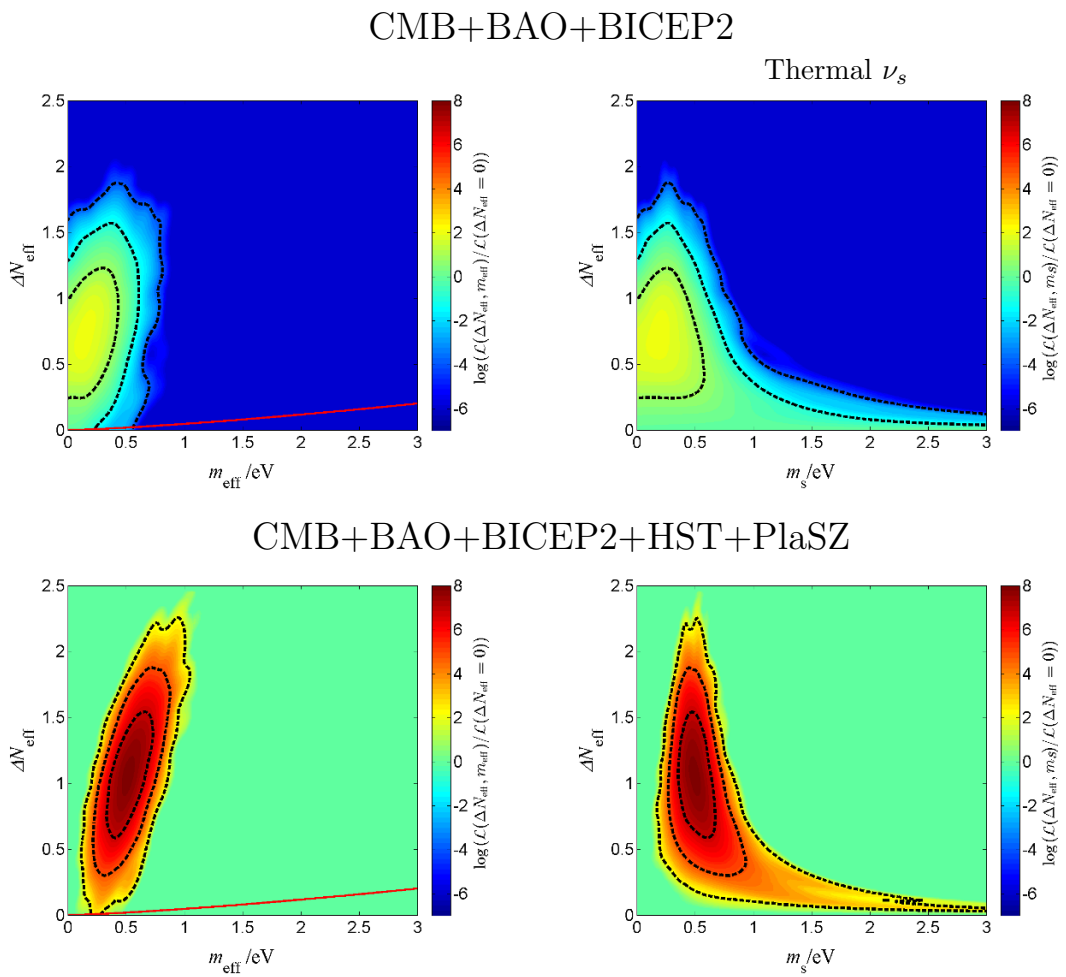

Figure 2. Same two upper panels in figure 1, but for CMB+BAO+BICEP2 cosmological data (*SET 2*, upper panels), and CMB+BAO+BICEP2+HST+PlaSZ cosmological data (*SET 3*, lower panels).

section. In doing so we are going to assume that the contribution of the sterile neutrino to the cosmological observables is independent of the active-sterile neutrino mixing (see discussion around eq. (3.2)). Under this assumption our tests will require the marginalized likelihood of the sterile neutrino mass m_s obtained from the analysis of the SBL anomalies in the 3+1 scenario (marginalized with respect to all other oscillation parameters in the scenario), and the marginalized likelihoods of $(m_s, \Delta N_{\rm eff})$ from the cosmological analysis previously presented.

Concerning the SBL likelihood, we consider two different functions that can be interpreted as the two limiting cases. In the first, we consider the precise SBL likelihood as given in figure 1 in ref. [54] which we reproduce in figure 3 (in this case below roughly seven log-units from the maximum value, we set the SBL likelihood to a constant value). We label this case in the following as "full SBL likelihood". In the second case, we approximate the SBL likelihood as a top-hat shaped likelihood which is constant and non-zero between 0.86 eV and 1.57 eV and zero otherwise (which we illustrate by the arrow in figure 3). This is what we label in the following as "box SBL likelihood".

JHEP10(2014)104

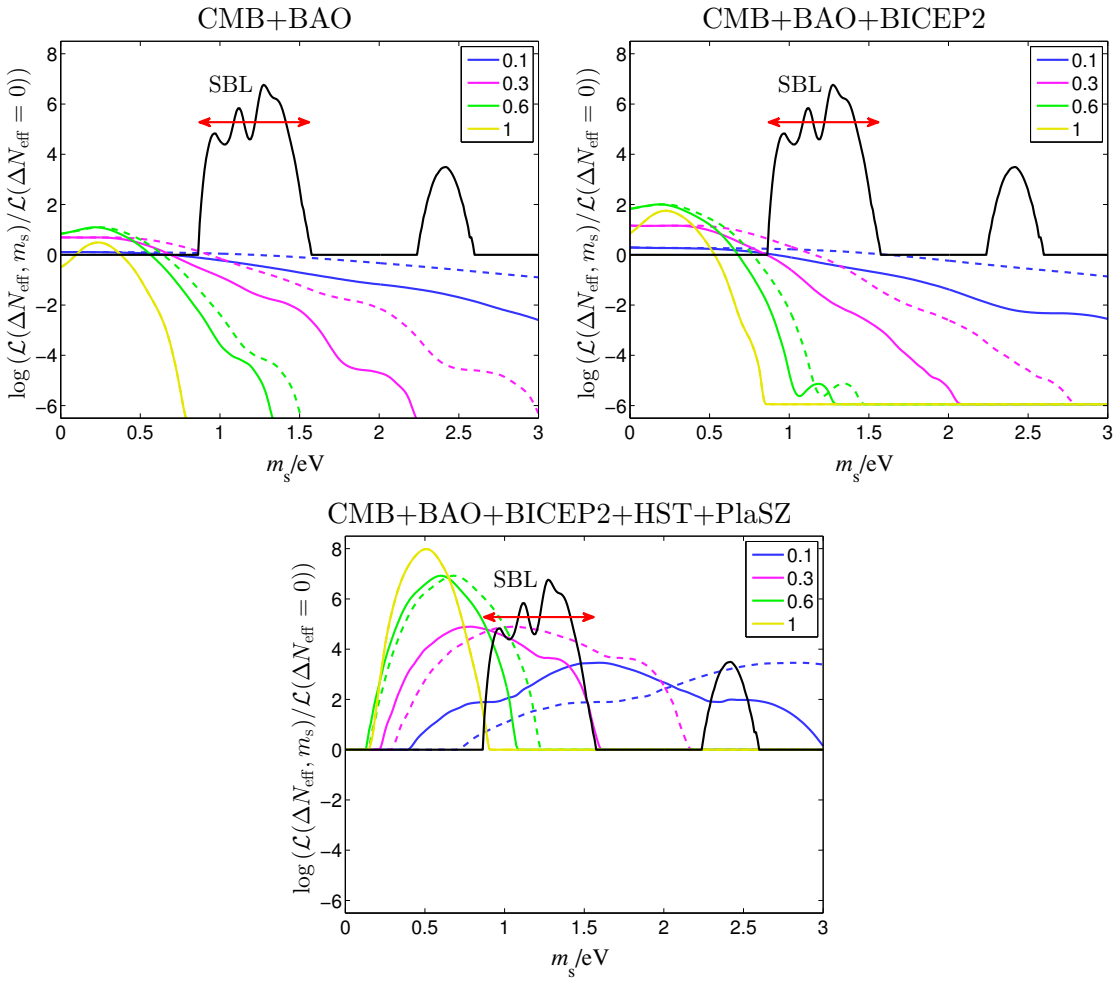

Figure 3. Marginal likelihoods as function of m_s for fixed $\Delta N_{\rm eff}$ ($\Delta N_{\rm eff} = 0.1, 0.3, 0.6, 1$) and for thermal ν_s (solid lines) and for the DW scenario (dashed lines). We show the results for the three cosmological data sets used as labeled in the figure. In all panels we also include the marginal likelihood for the SBL analysis in the 3+1 scenario (marginalized with respect to the lighter neutrino masses and all mixings) as given in figure 1 in ref. [54]. We denote by the red arrow the width and height of the box used to define "box SBL likelihood" (see text for details).

4.1 Sterile neutrinos vs none

The first question we want to address is whether the current data shows evidence of the existence of sterile neutrinos, and how strong this evidence is. Generically in Bayesian analyses this takes the form of model comparison between a model without sterile neutrinos and a model with sterile neutrinos using some posterior odds, eq. (2.2). There are several ways to go about answering this question. In here we are interested in testing what cosmology has to say on this comparison for the sterile models invoked to explain the SBL anomalies. This is, in this case the first model H_0 is defined as a model with no sterile neutrino, which implies a cosmological model with $\Delta N_{\rm eff} = 0$. And the other model, H_1 is taken to include one sterile neutrino of mass $m_{\rm s}$ *as required to accommodate the SBL*

JHEP10(2014)104

anomalies and which contributes to relativistic energy density in the early Universe as some fix $\Delta N_{\rm eff}$.

In this case we can define a posterior odds as:

$$\begin{aligned}\mathcal{O} &= \frac{\Pr(D_{\rm c}|D_{\rm SBL},H_1)}{\Pr(D_{\rm c}|D_{\rm SBL},H_0)}\frac{\Pr(H_1|D_{\rm SBL})}{\Pr(H_0|D_{\rm SBL})} \\ &= \frac{\Pr(D_{\rm c}|D_{\rm SBL},H_1)}{\Pr(D_{\rm c}|D_{\rm SBL},H_0)}\frac{\Pr(D_{\rm SBL}|H_1)}{\Pr(D_{\rm SBL}|H_0)}\frac{\Pr(H_1)}{\Pr(H_0)} \\ &\equiv \mathcal{B}_{10}^{\rm upd}\mathcal{B}_{10}^{\rm SBL}\frac{\Pr(H_1)}{\Pr(H_0)}\,,\end{aligned} \tag{4.1}$$

with

$$\mathcal{B}_{10}^{\rm SBL} \equiv \frac{\Pr(D_{\rm SBL}|H_1)}{\Pr(D_{\rm SBL}|H_0)} \tag{4.2}$$

and

$$\mathcal{B}_{10}^{\rm upd} \equiv \frac{\Pr(D_{\rm c}|D_{\rm SBL},H_1)}{\Pr(D_{\rm c}|D_{\rm SBL},H_0)} = \frac{\Pr(D_{\rm c}|D_{\rm SBL},H_1)}{\Pr(D_{\rm c}|H_0)} = \frac{\Pr(D_{\rm c},D_{\rm SBL}|H_1)}{\Pr(D_{\rm c}|H_0)\Pr(D_{\rm SBL}|H_1)}\,, \tag{4.3}$$

where in the last line we have used that SBL is not sensitive to any parameters effecting cosmology once we assume that there are no sterile neutrinos and hence $D_{\rm SBL}$ and $D_{\rm c}$ are independent under H_0. The quantity $\mathcal{B}_{10}^{\rm upd}$ quantifies how much better the prediction of cosmological data assuming sterile neutrino and SBL data is than the prediction assuming no sterile neutrinos.

Now, the model H_1 is inherently more complex than H_0 since it contains additional parameters (sterile mass and mixings), and this is as usual compensated for in a Bayesian analysis. In the first row of eq. (4.1) this is contained in the last factor of $\Pr(H_1|D_{\rm SBL})/\Pr(H_0|D_{\rm SBL}) = \mathcal{B}_{10}^{\rm SBL}\frac{\Pr(H_1)}{\Pr(H_0)}$. Now, the best-fit of the SBL data is significantly better if you have a sterile neutrino, but because of the added complexity it might not be totally unreasonable to have $\Pr(H_1|D_{\rm SBL})/\Pr(H_0|D_{\rm SBL}) = \mathcal{O}(1)$.

In any case, it is the first factor in eq. (4.1) the factor by which the cosmological data have *updated* the SBL-only posterior odds to the final SBL+cosmology odds and which we will be using in our quantification. Furthermore, under the additional assumption that $\Delta N_{\rm eff}$ is unconstrained by SBL data, $\Pr(D_{\rm SBL}|H_1)$ does not depend on $\Delta N_{\rm eff}$, and hence $\mathcal{B}_{10}^{\rm upd}$ is in fact simply proportional to the combined marginal likelihood of $\Delta N_{\rm eff}$, normalized such that $\mathcal{B}_{10}^{\rm upd} = 1$ for $\Delta N_{\rm eff} = 0$.

Before discussing the results, let us mention that here, as in any Bayesian analysis, the results are in principle always prior dependent, and we should consider how large this dependence is in practice. First, as discussed in section 3, the marginal likelihood depends on the priors on the cosmological nuisance parameters, but this dependence is expected to be small (except possibly for r). More significantly, there is the dependence of the total Bayes factor and odds on the prior on m_s, even when it is well constrained by the combined data set. However the value of $\mathcal{B}_{10}^{\rm upd}$ does not strongly depend on the shape of the prior nor its upper limit. This is so because the well-constraining SBL data is used to update the

JHEP10(2014)104

prior to a posterior (which is rather insensitive to the prior) which is then used to analyze the cosmological data. We use a uniform prior between 0 and 10 eV as the nominal upper limit, since, as described in ref. [38], this roughly defines the region where (for the CMB) the particles are distinct from cold or warm dark matter.

The results are shown in the left panel of figure 4. We see that for the CMB+BAO and CMB+BAO+BICEP2 data sets, $\mathcal{B}_{10}^{\rm upd}$ decreases quite steadily with $\Delta N_{\rm eff}$. These cosmological data hence disfavour models with sterile neutrinos required to explain the SBL anomalies over the model without sterile neutrinos, independently of how much the contribution of the sterile neutrino to the energy density is suppressed with respect to the fully thermalized expectation. We also see that the addition of the BICEP2 data has a small impact on these conclusions.

For the CMB+BAO+BICEP2+HST+PlaSZ data set, there is, on the contrary, a significant peak for intermediate values of $\Delta N_{\rm eff}$. The ΛCDM+r model is significantly disfavoured by this combination of cosmological data, while increasing $\Delta N_{\rm eff}$ increases the cosmological likelihood for SBL-compatible masses. However, further increasing $\Delta N_{\rm eff}$, cosmology requires a too small mass, so the $\mathcal{B}_{10}^{\rm upd}$ decrease again. Notice also that in fact the ΛCDM+r is so disfavored that it is in the region where the (too large) constant extrapolation is used. Hence, the exact $\mathcal{B}_{10}^{\rm upd}$ is expected to be even larger.

4.2 Consistency of parameter constraints

In addition to comparing the models with and without sterile neutrinos we now address the question of the consistency of the parameter constraints from the different data sets within the 3+1 model. A Bayesian test was formulated in [88], in which a model where both data sets are fitted by the same physical parameters is compared with a model in which each data set uses their own parameters. However, as is often the case in model comparison, the result can depend crucially on the prior on the parameters, in our case m_s in particular. Since we cannot motivate using a specific shape or limits on the prior, we instead use the corresponding χ^2-test (these were also compared in [88]). Although not rigorous as the Bayesian test, it has the clear advantage that it is prior-independent.

In particular, if we want to test how inconsistent the constraints on the sterile mass from the different data sets are once a certain $\Delta N_{\rm eff}$ is assumed, i.e., without considering how favoured or disfavoured that $\Delta N_{\rm eff}$ is by the cosmological data, we should evaluate

$$\Delta\chi^2(\Delta N_{\rm eff}) = \hat{\chi}^2_{\rm comb}(\Delta N_{\rm eff}) - \hat{\chi}^2_{\rm SBL} - \hat{\chi}^2_{\rm cosmo}(\Delta N_{\rm eff}) \,, \tag{4.4}$$

where the hat denotes the value at the best fit i.e., optimized over m_s ($\chi^2_{\rm SBL}$ does not depend on $\Delta N_{\rm eff}$).

The results of this test are shown on the right-hand side of figure 4. As expected, the results for CMB+BAO and CMB+BAO+BICEP2 are quite similar and show an steady increase of the inconsistency with $\Delta N_{\rm eff}$. Also comparing the DW and thermal scenarios, we see that in general, to obtain the same $\Delta\chi^2$, larger values of $\Delta N_{\rm eff}$ are required in the DW scenario. This is so because, as explained before, in the DW scenario the preferred masses are shifted to larger values by an amount which increases as $\Delta N_{\rm eff} < 1$ decreases.

JHEP10(2014)104

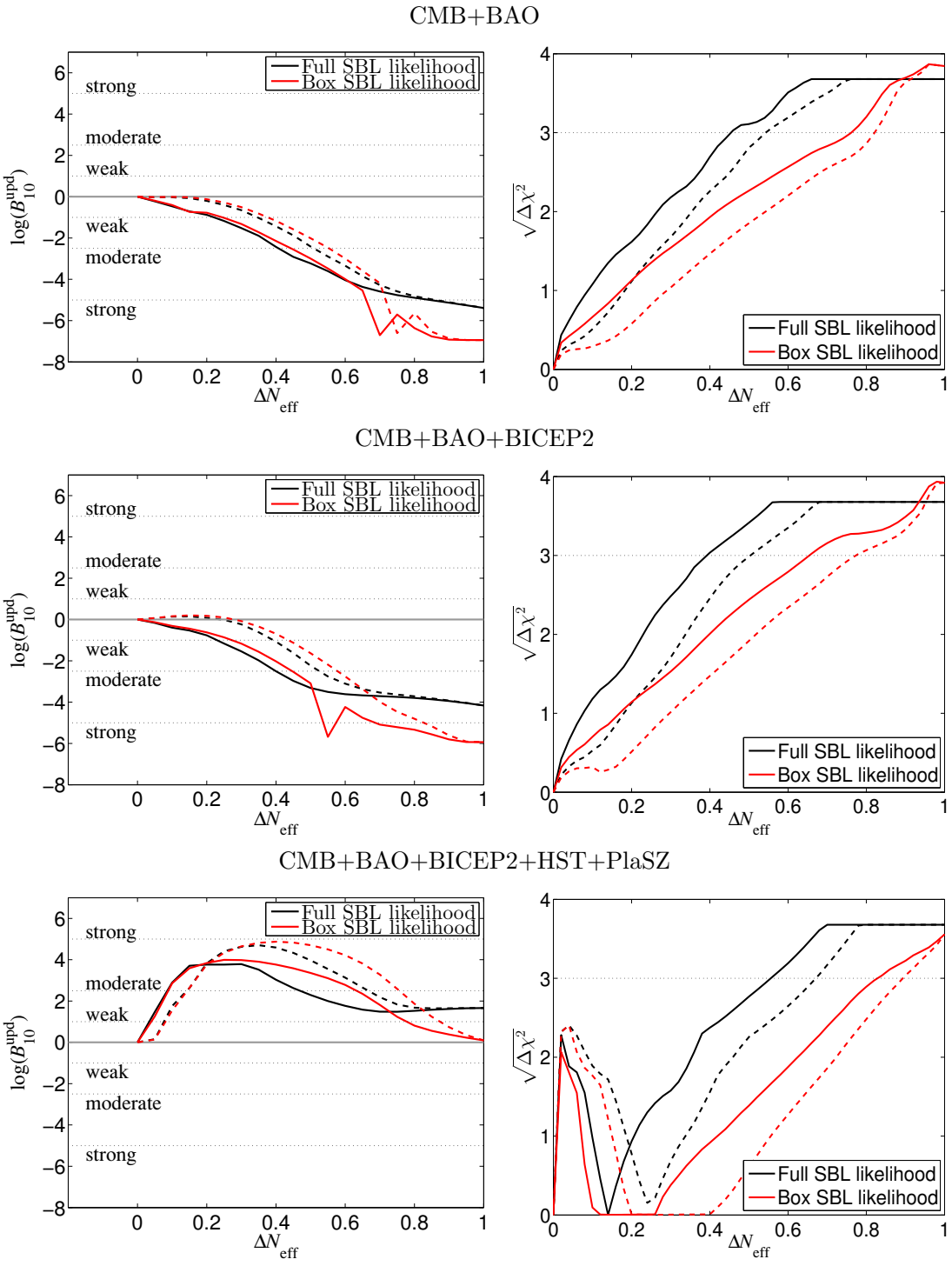

Figure 4. Left panels: logarithm of the Bayes factor $\mathcal{B}_{10}^{\rm upd}$ as a function of $\Delta N_{\rm eff}$. Right panels: consistency of mass constraints. In all panels the results are shown for thermal ν_s (solid lines) and for the DW scenario (dashed lines) and for the SBL full (black) and Box likelihood (red). We show the results for the three cosmological data sets considered: CMB+BAO (upper row), CMB+BAO+BICEP2 (middle row), CMB+BAO+BICEP2+HST+PlaSZ (lower row).

JHEP10(2014)104

As for the results for the box and full SBL likelihoods, we notice that, typically, using the full SBL likelihood gives a larger inconsistency. This is because the box likelihood is constant over a wide range of m_s, and over this wide range the cosmological likelihood typically varies significantly. The combined χ^2 can then easily be reduced by finding the best fit within this range.

For the CMB+BAO+BICEP2+HST+PlaSZ combination, one observes in each curve a peak for small value of $\Delta N_{\rm eff}$, although it does not reach the level of 2.5σ. These peaks are due to the fact that (cf. figure 2) cosmology prefers large physical masses, too large to fit the SBL data. As $\Delta N_{\rm eff}$ increases, the mass constraints become compatible, but as $\Delta N_{\rm eff}$ continues to decrease, cosmology requires the masses to be smaller than those which can fit the SBL data and the inconsistency increases.

Again, we stress that this consistency test is in principle not affected by how favoured or disfavoured the considered value of $\Delta N_{\rm eff}$ is, but instead consider that value to be "true", and then test the compatibility of the constraints on the mass. For example, comparing the left and right panels in the last raw of figure 4 we see that for the CMB+BAO+BICEP2+HST+PlaSZ data set, even though from the right panel we read that the mass ranges required for cosmology and SBL become highly incompatible for $\Delta N_{\rm eff}$ close to one, from the left hand side we see that these large values of $\Delta N_{\rm eff}$ are not particularly disfavoured compared to small $\Delta N_{\rm eff}$, for which the mass constraints are compatible. So what we see is that large $\Delta N_{\rm eff}$ is disfavoured because the sterile mass required by SBL and cosmology are incompatible, and small $\Delta N_{\rm eff}$ is disfavoured because it is so in the cosmological (and consequently in the combined) analysis. So small and large $\Delta N_{\rm eff}$ have comparable Bayes factors, but this is only because they are both disfavoured.

5 Summary

In this paper we have revisited the question of the information which cosmology provides on the scenarios with $\mathcal{O}(\text{eV})$ mass sterile neutrinos invoked to explain the SBL anomalies (eq. (1)) using Bayesian statistical tests and study how the results depend on the inclusion of the recently CMB polarization results of BICEP2 and on the inclusion of local measurements which show some tension with the Planck and LSS-BAO results when analyzed in the framework of the ΛCDM scenario.

In order to do so we have first performed an analysis of three characteristic sets of cosmological data in $\Lambda\text{CDM}+r+\nu_s$ cosmologies as described in section 3. The result of our analysis is presented in figures 1 and 2 in the form of marginalized cosmological likelihoods in terms of the two relevant parameters, the sterile neutrino mass m_s and its contribution to the energy density of the early Universe $\Delta N_{\rm eff}$. The results clearly indicate that, as long as the HST and SZ cluster data from Planck are not included, cosmological data favours the sterile neutrino mass m_s clearly well below eV unless its contribution to the energy density is suppressed with respect to the expected from a fully thermalized sterile neutrino. The inclusion of the BICEP2 data does not substantially affect this conclusion. Conversely, including these HST and SZ cluster data, higher sterile masses become favoured.

JHEP10(2014)104

Evidence	Scenario /SBL Likel	SET 1 3+1 Disfavoured	SET 2 3+1 Disfavoured	SET 3 3+1 Favoured
Weak	TH/FULL	$[0.22, 0.40]$	$[0.23, 0.40]$	$[0.03, 0.08] \oplus \geq 0.47$
	TH/BOX	$[0.25, 0.44]$	$[0.27, 0.45]$	$[0.04, 0.09] \oplus [0.63, 0.78]$
	DW/FULL	$[0.35, 0.51]$	$[0.39, 0.52]$	$[0.08, 0.14] \oplus \geq 0.67$
	DW/BOX	$[0.38, 0.55]$	$[0.44, 0.58]$	$[0.08, 0.14] \oplus [0.76, 0.87]$
Moderate	TH/FULL	$[0.40, 0.86]$	≥ 0.40	$[0.08, 0.47]$
	TH/BOX	$[0.44, 0.66]$	$[0.45, 0.53] \oplus [0.57, 0.68]$	$[0.09, 0.63]$
	DW/FULL	$[0.51, 0.86]$	≥ 0.52	$[0.14, 0.67]$
	DW/BOX	$[0.55, 0.72]$	$[0.58, 0.83]$	$[0.14, 0.76]$
Strong	TH/FULL	≥ 0.86	—	—
	TH/BOX	≥ 0.66	$[0.53, 0.57] \oplus \geq 0.68$	–
	DW/FULL	≥ 0.86	—	–
	DW/BOX	≥ 0.72	≥ 0.83	—

Table 3. Ranges of $\Delta N_{\rm eff}$ for which we find the evidence against or in favour of the 3+1 model compared to the model with only the 3 active neutrinos to be weak, moderate or strong.

With these results, we have performed in section 4 two statistical test on their (in)compatibility with the corresponding likelihood derived from the analysis of the SBL results as given in ref. [54]. In the first test we have asked ourselves whether cosmology favours or disfavours the 3+1 sterile models which explain the SBL results over a model without sterile neutrinos. In order to do so we have constructed the Bayes factor defined in eq. (4.3) which gives the factor by which the cosmological data *updates* the SBL-only posterior odds of the 3+1 vs 3+0 model to the final SBL+cosmology odds and we have studied its behaviour as a function of $\Delta N_{\rm eff}$. The results of this test, shown in figure 4, implies that, as long as the HST and SZ cluster data from Plank is not included, the cosmological analysis disfavour the 3+1 model with respect to 3+0. The inclusion of these cosmological data however favours the 3+1 model for an intermediate range of $\Delta N_{\rm eff}$. We summarize in table 3 the ranges of $\Delta N_{\rm eff}$ for which we find the evidence against or in favour of the 3+1 model compared to the model with only the 3 active neutrinos to be weak, moderate or strong from these analyses.

The second test performed deals with the (in)compatibility of the sterile mass constraints as required to describe SBL and cosmology. For this we have evaluated the $\Delta\chi^2$ defined in eq. (4.4) which we plot in the right panels in figure 4. Altogether we read that this test yields inconsistency on the m_s required by cosmology and SBL larger than 3σ for

$$\begin{aligned}
&\Delta N_{\rm eff} \geq 0.45\,(0.54)\,[0.76]\;([0.82]) \quad \text{For CMB + BAO}\,,\\
&\Delta N_{\rm eff} \geq 0.39\,(0.50)\,[0.65]\;([0.77]) \quad \text{For CMB + BAO + BICEP2}\,,\\
&\Delta N_{\rm eff} \geq 0.56\,(0.67)\,[0.83]\;([0.89]) \quad \text{For CMB + BAO + BICEP2 + HST + PlaSZ}\,,
\end{aligned} \tag{5.1}$$

for thermal (WP) ν_s scenario for the full [box] SBL likelihood.

In summary, we find that the analysis of cosmological results from temperature and polarization data on the CMB as well as from the BAO measurements from LSS data disfavours the 3+1 sterile models introduced to explain the SBL anomalies over the scenario

JHEP10(2014)104

without sterile neutrinos, and also that their allowed/required ranges of m_s are incompatible. This is so even if new physics is involved so that the contribution of the sterile neutrino to the energy density of the Universe (and therefore to the cosmological observables) is suppressed with respect to that of the fully thermalized case resulting from its mixing with the active neutrinos. When the local measurement of the H_0 by the Hubble Space Telescope, and the cluster SZ cluster data from the Planck mission is included, compatibility can be found between cosmological and SBL data, but still requires a substantial suppression of the ν_s contribution to ρ_R.

Acknowledgments

This work is supported by USA-NSF grants PHY-09-69739 and PHY-1316617, by CUR Generalitat de Catalunya grant 2009SGR502 by MICINN FPA2010-20807 and consolider-ingenio 2010 program grants CUP (CSD-2008-00037) and CPAN, and by EU grant FP7 ITN INVISIBLES (Marie Curie Actions PITN-GA-2011-289442). J.S. acknowledges support from the Wisconsin IceCube Particle Astrophysics Center (WIPAC) and U. S. Department of Energy under the contract DE-FG-02-95ER40896.

References

[1] B. Pontecorvo, *Neutrino experiments and the problem of conservation of leptonic charge*, *Sov. Phys. JETP* **26** (1968) 984 [INSPIRE].

[2] V.N. Gribov and B. Pontecorvo, *Neutrino astronomy and lepton charge*, *Phys. Lett.* **B 28** (1969) 493 [INSPIRE].

[3] M.C. Gonzalez-Garcia and M. Maltoni, *Phenomenology with massive neutrinos*, *Phys. Rept.* **460** (2008) 1 [arXiv:0704.1800] [INSPIRE].

[4] M.C. Gonzalez-Garcia, M. Maltoni, J. Salvado and T. Schwetz, *Global fit to three neutrino mixing: critical look at present precision*, *JHEP* **12** (2012) 123 [arXiv:1209.3023] [INSPIRE].

[5] K.N. Abazajian et al., *Light sterile neutrinos: a white paper*, arXiv:1204.5379 [INSPIRE].

[6] LSND collaboration, A. Aguilar-Arevalo et al., *Evidence for neutrino oscillations from the observation of anti-neutrino(electron) appearance in a anti-neutrino(muon) beam*, *Phys. Rev.* **D 64** (2001) 112007 [hep-ex/0104049] [INSPIRE].

[7] MiniBooNE collaboration, A.A. Aguilar-Arevalo et al., *Event excess in the MiniBooNE search for $\bar{\nu}_\mu \to \bar{\nu}_e$ oscillations*, *Phys. Rev. Lett.* **105** (2010) 181801 [arXiv:1007.1150] [INSPIRE].

[8] MiniBooNE collaboration, A.A. Aguilar-Arevalo et al., *Improved search for $\bar{\nu}_\mu \to \bar{\nu}_e$ oscillations in the MiniBooNE experiment*, *Phys. Rev. Lett.* **110** (2013) 161801 [arXiv:1207.4809] [INSPIRE].

[9] G. Mention et al., *The reactor antineutrino anomaly*, *Phys. Rev.* **D 83** (2011) 073006 [arXiv:1101.2755] [INSPIRE].

JHEP10(2014)104

[10] T. Mueller et al., *Improved predictions of reactor antineutrino spectra*, *Phys. Rev.* **C 83** (2011) 054615 [arXiv:1101.2663] [INSPIRE].

[11] P. Huber, *On the determination of anti-neutrino spectra from nuclear reactors*, *Phys. Rev.* **C 84** (2011) 024617 [*Erratum ibid.* **C 85** (2012) 029901] [arXiv:1106.0687] [INSPIRE].

[12] C. Giunti and M. Laveder, *Statistical significance of the Gallium anomaly*, *Phys. Rev.* **C 83** (2011) 065504 [arXiv:1006.3244] [INSPIRE].

[13] C. Giunti, M. Laveder, Y.F. Li, Q.Y. Liu and H.W. Long, *Update of short-baseline electron neutrino and antineutrino disappearance*, *Phys. Rev.* **D 86** (2012) 113014 [arXiv:1210.5715] [INSPIRE].

[14] M.A. Acero, C. Giunti and M. Laveder, *Limits on ν_e and $\bar{\nu}_e$ disappearance from Gallium and reactor experiments*, *Phys. Rev.* **D 78** (2008) 073009 [arXiv:0711.4222] [INSPIRE].

[15] J. Kopp, M. Maltoni and T. Schwetz, *Are there sterile neutrinos at the eV scale?*, *Phys. Rev. Lett.* **107** (2011) 091801 [arXiv:1103.4570] [INSPIRE].

[16] C. Giunti and M. Laveder, *$3+1$ and $3+2$ sterile neutrino fits*, *Phys. Rev.* **D 84** (2011) 073008 [arXiv:1107.1452] [INSPIRE].

[17] C. Giunti and M. Laveder, *Status of $3+1$ neutrino mixing*, *Phys. Rev.* **D 84** (2011) 093006 [arXiv:1109.4033] [INSPIRE].

[18] C. Giunti and M. Laveder, *Implications of $3+1$ short-baseline neutrino oscillations*, *Phys. Lett.* **B 706** (2011) 200 [arXiv:1111.1069] [INSPIRE].

[19] A. Donini, P. Hernández, J. Lopez-Pavon, M. Maltoni and T. Schwetz, *The minimal $3+2$ neutrino model versus oscillation anomalies*, *JHEP* **07** (2012) 161 [arXiv:1205.5230] [INSPIRE].

[20] J.M. Conrad, C.M. Ignarra, G. Karagiorgi, M.H. Shaevitz and J. Spitz, *Sterile neutrino fits to short baseline neutrino oscillation measurements*, *Adv. High Energy Phys.* **2013** (2013) 163897 [arXiv:1207.4765] [INSPIRE].

[21] C. Giunti, M. Laveder, Y.F. Li and H.W. Long, *Pragmatic view of short-baseline neutrino oscillations*, *Phys. Rev.* **D 88** (2013) 073008 [arXiv:1308.5288] [INSPIRE].

[22] G. Karagiorgi, M.H. Shaevitz and J.M. Conrad, *Confronting the short-baseline oscillation anomalies with a single sterile neutrino and non-standard matter effects*, arXiv:1202.1024 [INSPIRE].

[23] J. Kopp, P.A.N. Machado, M. Maltoni and T. Schwetz, *Sterile neutrino oscillations: the global picture*, *JHEP* **05** (2013) 050 [arXiv:1303.3011] [INSPIRE].

[24] Particle Data Group collaboration, K. Nakamura et al., *Review of particle physics*, *J. Phys.* **G 37** (2010) 075021 [INSPIRE].

[25] G. Mangano et al., *Relic neutrino decoupling including flavor oscillations*, *Nucl. Phys.* **B 729** (2005) 221 [hep-ph/0506164] [INSPIRE].

[26] N. Saviano et al., *Multi-momentum and multi-flavour active-sterile neutrino oscillations in the early universe: role of neutrino asymmetries and effects on nucleosynthesis*, *Phys. Rev.* **D 87** (2013) 073006 [arXiv:1302.1200] [INSPIRE].

[27] A. Mirizzi et al., *The strongest bounds on active-sterile neutrino mixing after Planck data*, *Phys. Lett.* **B 726** (2013) 8 [arXiv:1303.5368] [INSPIRE].

JHEP10(2014)104

[28] M.C. Gonzalez-Garcia, M. Maltoni and J. Salvado, *Robust cosmological bounds on neutrinos and their combination with oscillation results*, *JHEP* **08** (2010) 117 [arXiv:1006.3795] [INSPIRE].

[29] M.A. Acero and J. Lesgourgues, *Cosmological constraints on a light non-thermal sterile neutrino*, *Phys. Rev.* **D 79** (2009) 045026 [arXiv:0812.2249] [INSPIRE].

[30] J. Hamann, S. Hannestad, G.G. Raffelt, I. Tamborra and Y.Y.Y. Wong, *Cosmology seeking friendship with sterile neutrinos*, *Phys. Rev. Lett.* **105** (2010) 181301 [arXiv:1006.5276] [INSPIRE].

[31] E. Giusarma, M. Archidiacono, R. de Putter, A. Melchiorri and O. Mena, *Sterile neutrino models and nonminimal cosmologies*, *Phys. Rev.* **D 85** (2012) 083522 [arXiv:1112.4661] [INSPIRE].

[32] M. Archidiacono, E. Calabrese and A. Melchiorri, *The case for dark radiation*, *Phys. Rev.* **D 84** (2011) 123008 [arXiv:1109.2767] [INSPIRE].

[33] M. Archidiacono, N. Fornengo, C. Giunti and A. Melchiorri, *Testing* $3+1$ *and* $3+2$ *neutrino mass models with cosmology and short baseline experiments*, *Phys. Rev.* **D 86** (2012) 065028 [arXiv:1207.6515] [INSPIRE].

[34] M.C. Gonzalez-Garcia, V. Niro and J. Salvado, *Dark radiation and decaying matter*, *JHEP* **04** (2013) 052 [arXiv:1212.1472] [INSPIRE].

[35] P. Di Bari, S.F. King and A. Merle, *Dark radiation or warm dark matter from long lived particle decays in the light of Planck*, *Phys. Lett.* **B 724** (2013) 77 [arXiv:1303.6267] [INSPIRE].

[36] J. Hasenkamp and J. Kersten, *Dark radiation from particle decay: cosmological constraints and opportunities*, *JCAP* **08** (2013) 024 [arXiv:1212.4160] [INSPIRE].

[37] P. Graf and F.D. Steffen, *Dark radiation and dark matter in supersymmetric axion models with high reheating temperature*, *JCAP* **12** (2013) 047 [arXiv:1302.2143] [INSPIRE].

[38] PLANCK collaboration, P.A.R. Ade et al., *Planck 2013 results. XVI. Cosmological parameters*, *Astron. Astrophys.* (2014) [arXiv:1303.5076] [INSPIRE].

[39] S. Das et al., *The Atacama Cosmology Telescope: temperature and gravitational lensing power spectrum measurements from three seasons of data*, *JCAP* **04** (2014) 014 [arXiv:1301.1037] [INSPIRE].

[40] R. Keisler et al., *A measurement of the damping tail of the cosmic microwave background power spectrum with the South Pole Telescope*, *Astrophys. J.* **743** (2011) 28 [arXiv:1105.3182] [INSPIRE].

[41] C.L. Reichardt et al., *A measurement of secondary cosmic microwave background anisotropies with two years of South Pole Telescope observations*, *Astrophys. J.* **755** (2012) 70 [arXiv:1111.0932] [INSPIRE].

[42] BICEP2 collaboration, P.A.R. Ade et al., *Detection of B-mode polarization at degree angular scales by BICEP2*, *Phys. Rev. Lett.* **112** (2014) 241101 [arXiv:1403.3985] [INSPIRE].

[43] L. Verde, S.M. Feeney, D.J. Mortlock and H.V. Peiris, *(Lack of) cosmological evidence for dark radiation after Planck*, *JCAP* **09** (2013) 013 [arXiv:1307.2904] [INSPIRE].

[44] M. Archidiacono et al., *Light sterile neutrinos after BICEP-2*, *JCAP* **06** (2014) 031 [arXiv:1404.1794] [INSPIRE].

JHEP10(2014)104

[45] C. Dvorkin, M. Wyman, D.H. Rudd and W. Hu, *Neutrinos help reconcile Planck measurements with both Early and Local Universe*, *Phys. Rev.* **D 90** (2014) 083503 [arXiv:1403.8049] [INSPIRE].

[46] J.-F. Zhang, Y.-H. Li and X. Zhang, *Sterile neutrinos help reconcile the observational results of primordial gravitational waves from Planck and BICEP2*, arXiv:1403.7028 [INSPIRE].

[47] J.-F. Zhang, Y.-H. Li and X. Zhang, *Cosmological constraints on neutrinos after BICEP2*, *Eur. Phys. J.* **C 74** (2014) 2954 [arXiv:1404.3598] [INSPIRE].

[48] F. Wu, Y. Li, Y. Lu and X. Chen, *Cosmological parameter fittings with the BICEP2 data*, *Sci. China Phys. Mech. Astron.* **57** (2014) 1449 [arXiv:1403.6462] [INSPIRE].

[49] B. Leistedt, H.V. Peiris and L. Verde, *No new cosmological concordance with massive sterile neutrinos*, *Phys. Rev. Lett.* **113** (2014) 041301 [arXiv:1404.5950] [INSPIRE].

[50] E. Giusarma, E. Di Valentino, M. Lattanzi, A. Melchiorri and O. Mena, *Relic neutrinos, thermal axions and cosmology in early 2014*, *Phys. Rev.* **D 90** (2014) 043507 [arXiv:1403.4852] [INSPIRE].

[51] R. Flauger, J.C. Hill and D.N. Spergel, *Toward an understanding of foreground emission in the BICEP2 region*, *JCAP* **08** (2014) 039 [arXiv:1405.7351] [INSPIRE].

[52] PLANCK collaboration, R. Adam et al., *Planck intermediate results. XXX. The angular power spectrum of polarized dust emission at intermediate and high Galactic latitudes*, arXiv:1409.5738 [INSPIRE].

[53] J. Hamann, S. Hannestad, G.G. Raffelt and Y.Y.Y. Wong, *Sterile neutrinos with eV masses in cosmology: how disfavoured exactly?*, *JCAP* **09** (2011) 034 [arXiv:1108.4136] [INSPIRE].

[54] J.R. Kristiansen, Ø. Elgarøy, C. Giunti and M. Laveder, *Cosmology with sterile neutrino masses from oscillation experiments*, arXiv:1303.4654 [INSPIRE].

[55] M. Archidiacono, N. Fornengo, C. Giunti, S. Hannestad and A. Melchiorri, *Sterile neutrinos: cosmology versus short-baseline experiments*, *Phys. Rev.* **D 87** (2013) 125034 [arXiv:1302.6720] [INSPIRE].

[56] S. Gariazzo, C. Giunti and M. Laveder, *Light sterile neutrinos in cosmology and short-baseline oscillation experiments*, *JHEP* **11** (2013) 211 [arXiv:1309.3192] [INSPIRE].

[57] C.M. Ho and R.J. Scherrer, *Sterile neutrinos and light dark matter save each other*, *Phys. Rev.* **D 87** (2013) 065016 [arXiv:1212.1689] [INSPIRE].

[58] G. Gelmini, S. Palomares-Ruiz and S. Pascoli, *Low reheating temperature and the visible sterile neutrino*, *Phys. Rev. Lett.* **93** (2004) 081302 [astro-ph/0403323] [INSPIRE].

[59] R. Foot and R.R. Volkas, *Reconciling sterile neutrinos with big bang nucleosynthesis*, *Phys. Rev. Lett.* **75** (1995) 4350 [hep-ph/9508275] [INSPIRE].

[60] Y.-Z. Chu and M. Cirelli, *Sterile neutrinos, lepton asymmetries, primordial elements: how much of each?*, *Phys. Rev.* **D 74** (2006) 085015 [astro-ph/0608206] [INSPIRE].

[61] L. Bento and Z. Berezhiani, *Blocking active sterile neutrino oscillations in the early universe with a Majoron field*, *Phys. Rev.* **D 64** (2001) 115015 [hep-ph/0108064] [INSPIRE].

[62] B. Dasgupta and J. Kopp, *Cosmologically safe eV-scale sterile neutrinos and improved dark matter structure*, *Phys. Rev. Lett.* **112** (2014) 031803 [arXiv:1310.6337] [INSPIRE].

[63] S. Hannestad, R.S. Hansen and T. Tram, *How self-interactions can reconcile sterile neutrinos with cosmology*, *Phys. Rev. Lett.* **112** (2014) 031802 [arXiv:1310.5926] [INSPIRE].

JHEP10(2014)104

[64] R. Trotta, *Bayes in the sky: bayesian inference and model selection in cosmology*, *Contemp. Phys.* **49** (2008) 71 [arXiv:0803.4089] [INSPIRE].

[65] M. Hobson et. al., *Bayesian methods in cosmology*, Cambridge University Press, Cambridge U.K. (2010)

[66] F. Feroz et al., *Bayesian selection of sign(μ) within mSUGRA in global fits including WMAP5 results*, *JHEP* **10** (2008) 064 [arXiv:0807.4512] [INSPIRE].

[67] J. Bergström, *Bayesian evidence for non-zero θ_{13} and CP-violation in neutrino oscillations*, *JHEP* **08** (2012) 163 [arXiv:1205.4404] [INSPIRE].

[68] J. Bergström, *Combining and comparing neutrinoless double beta decay experiments using different nuclei*, *JHEP* **02** (2013) 093 [arXiv:1212.4484] [INSPIRE].

[69] H. Jeffreys, *Theory of probability*, Oxford University Press, Oxford U.K. (1961).

[70] R.E. Kass and A.E. Raftery, *Bayes factors*, *J. Am. Stat. Ass.* **90** (1995) 773.

[71] PLANCK collaboration, P.A.R. Ade et al., *Planck intermediate results. XVI. Profile likelihoods for cosmological parameters*, *Astron. Astrophys.* **566** (2014) A54 [arXiv:1311.1657] [INSPIRE].

[72] J.O. Berger, B. Liseo and R.L. Wolpert, *Integrated likelihood methods for eliminating nuisance parameters*, *Stat. Sci.* **14** (1999) 1.

[73] WMAP collaboration, C.L. Bennett et al., *Nine-year Wilkinson Microwave Anisotropy Probe (WMAP) observations: final maps and results*, *Astrophys. J. Suppl.* **208** (2013) 20 [arXiv:1212.5225] [INSPIRE].

[74] BOSS collaboration, L. Anderson et al., *The clustering of galaxies in the SDSS-III baryon oscillation spectroscopic survey: baryon acoustic oscillations in the data release 10 and 11 galaxy samples*, arXiv:1312.4877 [INSPIRE].

[75] SDSS collaboration, W.J. Percival et al., *Baryon acoustic oscillations in the Sloan Digital Sky Survey data release 7 galaxy sample*, *Mon. Not. Roy. Astron. Soc.* **401** (2010) 2148 [arXiv:0907.1660] [INSPIRE].

[76] N. Padmanabhan, X. Xu, D.J. Eisenstein, R. Scalzo, A.J. Cuesta et al., *A 2 per cent distance to $z = 0.35$ by reconstructing baryon acoustic oscillations — I. Methods and application to the Sloan Digital Sky Survey*, *Mon. Not. Roy. Astron. Soc.* **427** (2012) 2132 [arXiv:1202.0090] [INSPIRE].

[77] F. Beutler et al., *The 6dF galaxy survey: baryon acoustic oscillations and the local Hubble constant*, *Mon. Not. Roy. Astron. Soc.* **416** (2011) 3017 [arXiv:1106.3366] [INSPIRE].

[78] C. Blake et al., *The WiggleZ dark energy survey: mapping the distance-redshift relation with baryon acoustic oscillations*, *Mon. Not. Roy. Astron. Soc.* **418** (2011) 1707 [arXiv:1108.2635] [INSPIRE].

[79] A.G. Riess et al., *A 3% solution: determination of the Hubble constant with the Hubble Space Telescope and Wide Field Camera 3*, *Astrophys. J.* **730** (2011) 119 [*Erratum ibid.* **732** (2011) 129] [arXiv:1103.2976] [INSPIRE].

[80] PLANCK collaboration, P.A.R. Ade et al., *Planck 2013 results. XX. Cosmology from Sunyaev-Zeldovich cluster counts*, arXiv:1303.5080 [INSPIRE].

[81] J. Benjamin et al., *CFHTLenS tomographic weak lensing: quantifying accurate redshift distributions*, arXiv:1212.3327 [INSPIRE].

JHEP10(2014)104

[82] C. Heymans et al., *CFHTLenS tomographic weak lensing cosmological parameter constraints: mitigating the impact of intrinsic galaxy alignments*, arXiv:1303.1808 [INSPIRE].

[83] M. Kilbinger et al., *CFHTLenS: combined probe cosmological model comparison using 2D weak gravitational lensing*, *Mon. Not. Roy. Astron. Soc.* **430** (2013) 2200 [arXiv:1212.3338] [INSPIRE].

[84] S. Dodelson and L.M. Widrow, *Sterile-neutrinos as dark matter*, *Phys. Rev. Lett.* **72** (1994) 17 [hep-ph/9303287] [INSPIRE].

[85] A. Lewis and S. Bridle, *Cosmological parameters from CMB and other data: a Monte Carlo approach*, *Phys. Rev.* **D 66** (2002) 103511 [astro-ph/0205436] [INSPIRE].

[86] A. Lewis, A. Challinor and A. Lasenby, *Efficient computation of CMB anisotropies in closed FRW models*, *Astrophys. J.* **538** (2000) 473 [astro-ph/9911177] [INSPIRE].

[87] J.-F. Zhang, J.-J. Geng and X. Zhang, *Neutrinos and dark energy after Planck and BICEP2: data consistency tests and cosmological parameter constraints*, arXiv:1408.0481 [INSPIRE].

[88] P. Marshall, N. Rajguru and A. Slosar, *Bayesian evidence as a tool for comparing datasets*, *Phys. Rev.* **D 73** (2006) 067302 [astro-ph/0412535] [INSPIRE].

JHEP10(2014)104